Superlattices and Microstructures 52 (2012) 484–499

Contents lists available at SciVerse ScienceDirect

Superlattices and Microstructures

journal homepage: www.elsevier.com/locate/superlattices

# Current transport mechanisms in Ru/Pd/n-GaN Schottky barrier diodes and deep level defect studies

V. Rajagopal Reddy *, N. Nanda Kumar Reddy

*Department of Physics, Sri Venkateswara University, Tirupati 517 502, India*

ARTICLE INFO

*Article history:*
Received 21 January 2012
Received in revised form 13 May 2012
Accepted 5 June 2012
Available online 15 June 2012

*Keywords:*
Schottky barrier diodes
*I–V* and *C–V* characteristics
Gaussian distribution
Interface state density
Deep level transient spectroscopy

ABSTRACT

We have investigated the current transport mechanisms in Ru/Pd/n-GaN Schottky barrier diodes in the temperature range 105–405 K. The calculated barrier height and ideality factor are 0.27 eV and 3.93 at 105 K, and 0.75 eV and 1.29 at 405 K respectively, and it is observed that barrier height ($\Phi_{bo}$) decreases and the ideality factor ($n$) increases with decreasing temperature. The apparent barrier height and the ideality factor derived by using thermionic emission theory are found to be strongly temperature dependent. This behavior has been interpreted based on the assumption of a Gaussian distribution of barrier heights due to barrier height inhomogeneities that prevail at the metal–semiconductor interface. The linearity of the apparent barrier height ($\Phi_{bo}$) versus $1/2kT$ plot yields a mean barrier height ($\bar{\Phi}_{bo}$) of 0.89 eV and a standard deviation ($\sigma_o$) of 111 mV. A modified $\ln(I_0/T^2) - (q^2\sigma_0^2/2k^2T^2)$ versus 1000/T plot gives $\bar{\Phi}_{bo}$ ($T = 0$) and $A^*$ as 0.87 eV and 21.25 A/cm$^2$ K$^2$, respectively without using the temperature coefficient of the barrier heights. The interface state densities extracted for the Ru/Pd/n-GaN Schottky diode are in the range of $9.38 \times 10^{13}$ to $1.06 \times 10^{12}$ eV$^{-1}$ cm$^{-2}$ in the band gap below conduction band from $E_C$-0.14 to $E_C$-0.66 eV. Deep level transient spectroscopy (DLTS) results showed that the two deep level defects are observed in as-grown sample ($E_1$ and $E_2$) which have activation energies of $E_1 = 0.54$ eV and $E_2 = 0.68$ eV, suggest that $E_2$ level is most probably associated with $N_{Ga}$-related defect.



* Corresponding author.
*E-mail address:* reddy_vrg@rediffmail.com (V. Rajagopal Reddy).

0749-6036/$ - see front matter © 2012 Elsevier Ltd. All rights reserved.
http://dx.doi.org/10.1016/j.spmi.2012.06.004

## 1. Introduction

Gallium nitride (GaN) has attracted great interest for applications in high power and high frequency devices due to their superior physical properties such as the wide band gap, the high breakdown electric field and high electron saturated velocity [1]. The devices fabricated in these material systems include ultraviolet Schottky barrier photodetectors [2], heterojunction bipolar transistors [3], visible-light emitting diodes [4], metal–semiconductor field effect transistors [5], and high electron mobility transistors [6]. Contacts, both ohmic and Schottky are important for these device applications. However, the Schottky contacts on GaN with a high and ideal Schottky barrier height (SBH) and a low leakage current and their physical origin still have a serious technological concern and are still intensively studied [7–8].

Due to technological importance of Schottky barrier diodes, a full understanding of the nature of conduction mechanism is of great interest. In most of the previous investigations [9–11], the Schottky barrier height (SBH) was determined at room temperature by measuring the current–voltage ($I$–$V$) and capacitance–voltage ($C$–$V$) characteristics of the Schottky barrier diodes. Analysis of the $I$–$V$ and $C$–$V$ characteristics of the Schottky barrier diodes at room temperature only does not give detailed information about their conduction process or the nature of barrier formation at the metal/semiconductor (MS) interface. The temperature dependence of the $I$–$V$ and $C$–$V$ characteristics of Schottky diode formed on n-GaN allows us to understand the different aspects of the conduction mechanisms at the metal/GaN interface [12–13]. Furthermore, the series resistance ($R_S$) and interface states density ($N_{SS}$) considerably affect the forward bias $I$–$V$ characteristics. The effects of these parameters and temperature on $I$–$V$ characteristics of Schottky barrier diodes are still the object of investigation [14,15].

Several researchers have investigated the temperature dependent electrical characteristics of Schottky contacts with different metallization schemes on n-GaN in various temperature ranges [16–21]. For example, Benamara et al. [16] investigated the temperature-dependent electrical properties of Au Schottky contacts to n-GaN. They found that at lower temperature ($T \leqslant 200$ K), the diode conduction mechanism is thermionic field emission (TFE), while at higher temperature ($T \geqslant 200$ K) it is thermionic emission (TE). Dogan et al. [17] studied the current–voltage characteristics of Au/Ni/n-GaN Schottky contacts in the temperature range 40–320 K, and analyzed in terms of thermionic emission theory by incorporating the concept of barrier inhomogeneity at the MS interface through Gaussian distribution function. Suresh et al. [18] investigated the current–voltage–temperature ($I$–$V$–T) characteristics of Pd/n-GaN Schottky diodes in the temperature range 298–390 K. They found that the ideality factor and the reverse leakage current increases with temperature, suggested that the conduction mechanism is through trap-assisted tunneling process or deep center hopping conduction. Mtangi et al. [19] evaluated the temperature dependence of electrical parameters of Au/Ni/n-GaN Schottky contacts in the temperature range 60–320 K. They pointed out that the variation of the barrier height at high temperatures was due to barrier inhomogeneities at the MS contact. Siva Pratap Reddy et al. [20] have explained the temperature dependence of the electrical parameters of Ni/Pd/n-GaN Schottky barrier diodes on the basis of thermionic emission theory with double Gaussian distribution of barrier heights due to the barrier height inhomogeneiteies at the MS interface. Recently, Rao et al. [21] investigated the leakage current mechanisms across the Pt/Au Schottky contacts on Ga-polarity GaN using $I$–$V$ measurements in the temperature range from 200 to 375 K by thermionic emission and Frenkel Poole Emission (FPE) modes. They reported that the leakage current is due to the emission of electrons from a trapped state near the MS interface into or from a continuum of states which are associated with conductive dislocations.

The performance of the aforementioned GaN-based Schottky contacts was not only limited by the abnormal leakage currents under reverse-bias but also deep levels found within the GaN band gap. These deep levels have the capability to act as traps and/or generation-recombination centers that reduce device speed, gain and efficiency [22]. Therefore, an understanding of these deep level defects in GaN materials is vital for improving material quality as well as device performance [23]. Previously, a number of researchers used deep level transient spectroscopy (DLTS) technique to characterize electronic trap states in GaN grown by MOCVD and HVPE [24–26]. For example, Gotz et al. [24] reported two deep levels with activation energies 0.49 eV and 0.18 eV with trap concentrations

$(6.3 \pm 0.1) \times 10^{14}$ cm$^{-3}$ for $E_1$ and $(7 \pm 1) \times 10^{13}$ cm$^{-3}$ for $E_2$ level, respectively. Hacke et al. [25] employed transient capacitance spectroscopy techniques to characterize the majority carrier traps in unintentionally doped n-type GaN grown by HVPE. They reported that three majority carrier traps with activation energies of 0.264 ± 0.01, 0.58 ± 0.017 and 0.665 ± 0.017 eV occurred at discrete energies below the conduction band. Tokuda et al. [26] characterized electron traps in n-type GaN which was grown homoepitaxially by MOCVD on free standing GaN substrates. They suggested that the traps B1 ($E_C$-0.23 eV) and B2 ($E_C$-0.58 eV) might be assigned to the $V_N$–$V_{Ga}$ pair and $N_{Ga}$-related defect, respectively.

In this work, a detailed analysis of the *I–V* and *C–V* characteristics of Ru/Pd/n-GaN Schottky contacts has been carried out in the temperature range 105–405 K to clarify the origin of the anomalous behavior of temperature dependence of the Schottky diode parameters such as the SBH, ideality factor, Richardson's constant, series resistance ($R_S$) and interface states density ($N_{SS}$). These results have been explained on the basis of a thermionic emission (TE) mechanism with lateral inhomogeneities at the Ru/Pd/n-GaN interface. The deep level transient spectroscopy (DLTS) technique has also been employed to characterize the deep level defects in as-grown GaN layer.

## 2. Experimental details

The samples used in this investigation were Si-doped n-type GaN grown by metal organic chemical vapor deposition (MOCVD) on c-plane $Al_2O_3$ sapphire substrate. The Hall effect measurement revealed that the films have a carrier concentration of about $4.07 \times 10^{17}$ cm$^{-3}$. Before ohmic contact fabrication, the n-GaN wafer was ultrasonically degreased for 5 min in each step in warm trichloroethylene, acetone and methanol and then rinsed with de-ionized (DI) water. This was followed by boiling aquaregia [$HNO_3$·HCl = 1:3] surface treatment for 10 min to remove the surface oxides and then rinsed in DI water. For ohmic contacts, Ti (25 nm)/Al (100 nm) layers were deposited on a portion of the sample by electron beam evaporation system and then annealed at 650 °C for 3 min in $N_2$ ambient. Circular Schottky contacts of Pd (20 nm)/Ru (30 nm) with a diameter of 0.7 mm were fabricated through a stainless steel mask using electron beam evaporation. All evaporation processes were carried out in a vacuum coating unit at about $6 \times 10^{-6}$ mbar. Metal layer thickness as well as deposition rates were monitored with the help of a digital quartz crystal thickness monitor. The deposition rates were about 1–2 Å/s. Current–voltage (*I–V*) measurements of the devices were first measured using Keithley source measuring unit (Model No. 2400) in the temperature range 105 to 405 K by steps of 30 K in the dark. The capacitance–voltage (*C–V*) and DLTS measurements were carried out by automated DLS-83D deep level spectrometer (Semi Lab, lock-in-amplifier based system which facilitated measurement at pulse frequency in the mHz range).

## 3. Results and discussion

### 3.1. Temperature-dependent current–voltage (*I–V*) characteristics

The current–voltage (*I–V*) relation for a Schottky diode based on the thermionic emission (TE) theory is given by [27]

$$I = I_0 \exp\left(\frac{qV}{nkT}\right)\left[1 - \exp\left(\frac{-qV}{kT}\right)\right] \tag{1}$$

where $n$ is the ideality factor, $I_o$ is the saturation current and it is defined by

$$I_o = AA^*T^2 \exp\left(\frac{-q\Phi_{bo}}{kT}\right) \tag{2}$$

where the quantities $A$, $A^*$, $T$, $q$, $k$ and $\Phi_{bo}$ are the diode area, the effective Richardson constant of 26.4 Acm$^{-2}$ K$^{-2}$ for n-GaN, temperature in Kelvin, the electronic charge, Boltzmann's constant and the zero-bias barrier height. From Eq. (1), the ideality factor n can be written as

$$n = \frac{q}{kT}\left(\frac{dV}{d(\ln I)}\right) \tag{3}$$

here, the ideality factor, n, is introduced to take into account the deviation of the experimental *I–V* data from the ideal thermionic emission model and should be $n = 1$ for an ideal contact. Fig. 1 shows the semi-log forward and reverse-bias *I–V* characteristics of the Ru/Pd/n-GaN Schottky barrier diodes at different temperatures. It is observed that the leakage current increases with increase in temperature and is in the range $3.08 \times 10^{-8}$ A (at 105 K) to $4.22 \times 10^{-4}$ A (at 405 K) at −1V. The large reverse leakage current is observed at high temperatures, which is due to the trap-assisted tunneling [18, 28–30] or deep center hopping type conduction [18]. The zero-bias barrier height ($\Phi_{bo}$) and the ideality factor ($n$) with temperature are calculated using Eq. (2) and (3) for Ru/Pd/n-GaN Schottky barrier diode. The estimated values of the zero-bias barrier height and ideality factor are changed from 0.27 eV and 3.93 at 105 K to 0.75 eV and 1.29 at 405 K, respectively.

The variation of zero-bias barrier height ($\Phi_{bo}$) and ideality factor ($n$) as a function of temperature is shown in Fig. 2. From Fig. 2, it is clear that the apparent barrier height decreases with decrease in temperature and the corresponding values are 0.75 eV at 405 K and 0.27 eV at 105 K. A similar phenomenon was also observed by other researchers [17,31]. The decrease in barrier height with decreasing temperature is explained as an effect of the barrier height being non-homogeneous, i.e. the barrier consists of low barrier embedded on a uniform barrier with individual cross-sectional areas. The presence of laterally extended Schottky barrier height (SBH) inhomogeneities at the metal–semiconductor (MS) interface allows for electron transport to be treated by the parallel conduction model [32,33]. Under this situation, the current flowing through the barrier is assumed to be the sum of all the individual currents, $I_i$ flowing through individual patches, each of its own area $A_i$ and Schottky barrier height, $\Phi_i$ [33]

$$I(V) = \Sigma I_i = A^* T^2 \left[\exp\left(\frac{qV}{kT}\right) - 1\right] \Sigma \exp\left(\frac{-q\Phi_i}{kT}\right) A_i \tag{4}$$

In this case the current will be dominated by the low barrier regions as at low temperatures, carriers will not be having enough energy to cross over the high barrier regions and thus the measured zero bias barrier height is low at low temperatures. On the other hand, from Fig. 2 it is evident that the

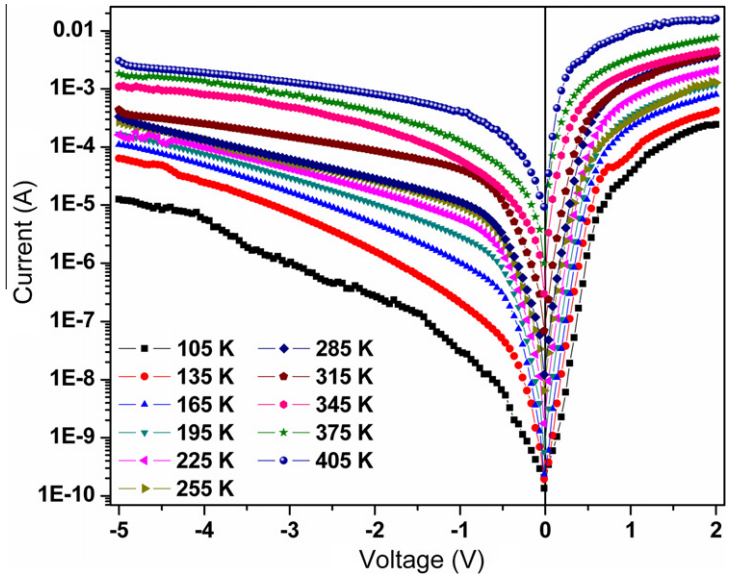


**Fig. 1.** Forward and reverse bias I-V characteristics for Ru/Pd/n-GaN Schottky diode in the temperature range of 105–405 K.

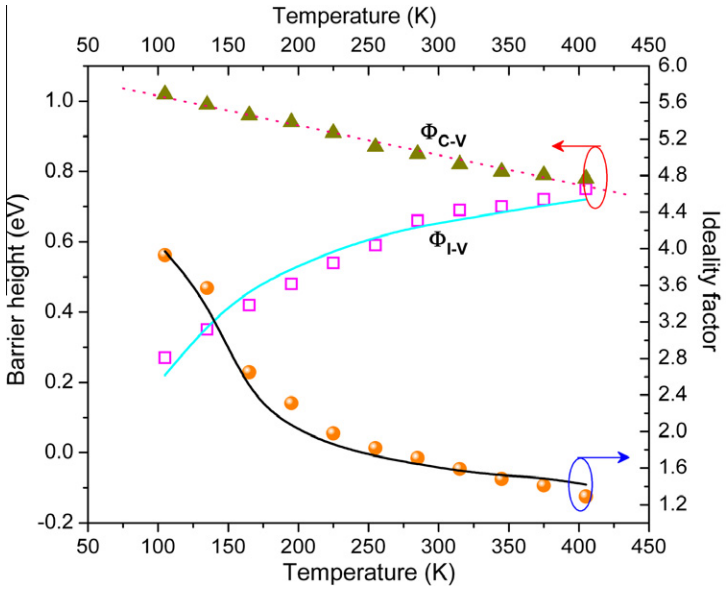


**Fig. 2.** Temperature dependence of the zero-bias apparent barrier height (the open squares) and ideality factor (the filled circles) for the Ru/Pd/n-GaN Schottky barrier diode. The continuous solid lines represent the estimated value of $\Phi_{ap}$ and $n_{ap}$ using Eqs. (11) and (12), respectively, for the Gaussian distributions of barrier height with $\bar{\Phi}_{bo}$ ($T$ = 0)=0.89 eV and $\sigma_o$ = 111 mV and $\rho_2$ = −0.132 V and $\rho_3$ = 0.012 V. The filled triangles indicate the SBH values obtained from the *C–V* method.

ideality factor n increases with decrease in temperature and its value increases from 1.29 at 405 K to 3.93 at 105 K. Similar trends have already been reported by other researchers [17,31]. The higher values of ideality factor at low temperatures indicate the presence of thermionic field emission (TFE) other than the pure thermionic emission [34]. The increase in ideality factor with decreasing temperature is known as $T_o$ effect [35]. The ideality factor ($n$) is found to be inversely proportional with temperature (figure not shown here) as

$$n(T) = n_o + \frac{T_o}{T} \tag{5}$$

where the $n_o$ and $T_o$ are constants which are found to be 0.32 and 394 K, respectively. Explanations of the possible origin of such case are proposed taking into account the interface state density distribution [36], quantum mechanical tunneling [27], and image force lowering [27]. One more reason to explain the deviation of ideality factor ($n$) values from unity at low temperatures could be due to the presence of generation-recombination centers. The recombination-generation current may arise from the defects such as deep levels in the forbidden gap of the GaN [16].

The influence of series resistance on the electrical characteristics of Ru/Pd/n-GaN Schottky diodes are investigated in the temperature range 105–405 K. The series resistance ($R_s$) is an important parameter of Schottky diodes. Generally, the forward bias *I–V* characteristics are linear on a semi-logarithmic scale at low forward bias voltages, but deviate significantly from linearity due to the effect of series resistance ($R_s$), the interfacial insulator layer and the interface states when the applied voltage is sufficiently large [37]. The series resistance is significant in downward curvature (non-linear region) of the forward-bias *I–V* characteristics, but the other two parameters ($\Phi_{bo}$ and $n$) are significant in both the linear and non-linear regions of the *I–V* characteristics. Lower the interface states density and the series resistance, the greater range over which the *I–V* curve (Fig. 1) yields a straight line [38]. The series resistance values are evaluated from the forward-bias *I–V* data using the method developed by Cheung and Cheung [39]. The forward-bias current–voltage characteristics due to thermionic emission of a Schottky contact with the series resistance can be expressed as Cheung's function

$$\frac{dV}{d(\ln I)} = IR_S + n\left(\frac{kT}{q}\right) \tag{6}$$

Fig. 3 shows the plots of experimental dV/d(ln I) versus I for different temperatures. Eq. (6) should give straight line for the data of downward curvature region in the forward bias *I–V* characteristics. Thus, a plot of dV/d(lnI) versus I will give $R_s$ as the slope and n(kT/q) as the *y*-axis intercept. Thus, for each temperature the values of series resistance ($R_s$) are calculated from Eq. (6) and the values are given in Table 1. It is clear that the series resistance ($R_s$) decreases more rapidly at high temperatures than at low temperatures. The increase of $R_s$ with the fall of temperature for the Ru/Pd/n-GaN sample is believed to arise from the factors responsible for increase of ideality factor and/or lack of free carrier concentration at low temperatures [40].

As an alternative method, an activation energy plot is used to determine the SBH and the Richardson constant. From the experimental data reported in Fig. 1, the value of the saturation current $I_o$ is determined at each temperature and conventional Richardson plot of $\ln(I_o/T^2)$ versus 1000/T is drawn for Ru/Pd/n-GaN SBDs and is shown (open squares) in Fig. 4. This activation energy plot of $\ln(I_o/T^2)$ versus 1000/T allows the determination of the effective SBH according to Eq. (2). An experimental $\ln(I_o/T^2)$ versus 1000/T plot should give a straight line with a slope given by a SBH $\Phi_{bo}$ ($T = 0$ K) and an intercept at the ordinate given by an experimental Richardson's constant, A*. When trying to fit the experimental data, a distortion of the curve is clearly visible at low temperatures. From this fit, a SBH $\Phi_{bo}$ ($T = 0$ K) of 0.49 eV and Richardson's constant value of $A^* = 23 \times 10^{-3}$ $Acm^{-2}$ $K^{-2}$ are extracted for Ru/Pd/n-GaN SBDs. Thus, the Richardson constant obtained from the conventional Richardson plot is typically much smaller than the theoretical value of 26.4 $Acm^{-2}K^{-2}$. Similar results have also been found by several authors [41,42]. Hacke et al. [41] suggested that it was caused by the presence of a barrier through which the electron must tunnel. The other possible reason for the low value of $A^*$ was due to the decrease of the effective contact area [42]. Moreover, non-linearity of the experimental $\ln(I_o/T^2)$ versus 1000/T curve may be caused by the temperature dependence of the BH and ideality factor due to the existence of the surface inhomogeneities of the GaN substrate [43].

The ideality factor is simply a manifestation of the barrier uniformity and it increases for an inhomogeneous barrier [44]. It is noted that a significant decrease in the zero-bias BH and increase in the ideality factor especially at low temperature. This is possibly caused by the barrier height inhomoge-

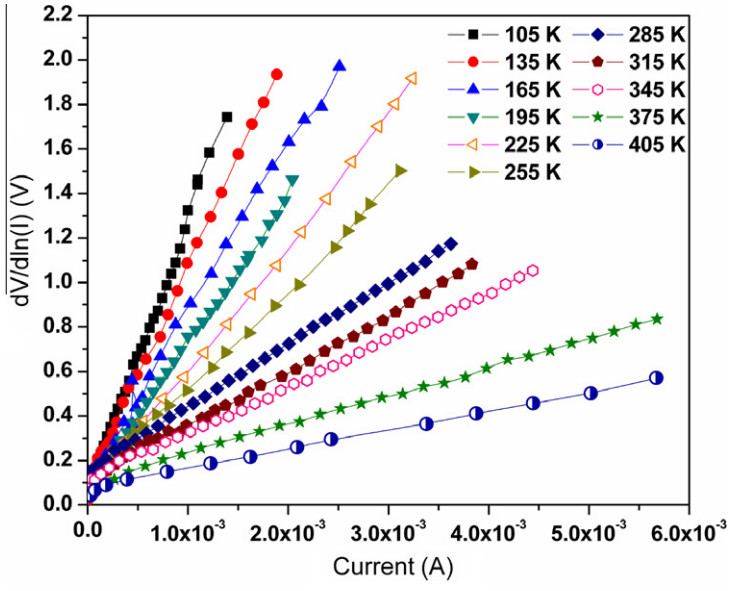


**Fig. 3.** Pot of dV/d(lnI) versus I for Ru/Pd/n-GaN Schottky diode at various temperatures.

**Table 1**
The temperature-dependent electrical parameters of Ru/Pd/n-GaN Schottky barrier diodes in the temperature range of 105–405 K.

| Temperature ($K$) | Ideality factor '$n$' | Barrier height (eV) | | Series resistance ($\Omega$) |
|---|---|---|---|---|
| | | $\Phi_{I-V}$ | $\Phi_{C-V}$ | |
| 105 | 3.93 | 0.27 | 1.02 | 1027 |
| 135 | 3.57 | 0.35 | 0.99 | 988 |
| 165 | 2.65 | 0.42 | 0.96 | 769 |
| 195 | 2.31 | 0.48 | 0.94 | 666 |
| 225 | 1.98 | 0.54 | 0.91 | 559 |
| 255 | 1.82 | 0.59 | 0.87 | 446 |
| 285 | 1.71 | 0.66 | 0.85 | 285 |
| 315 | 1.59 | 0.69 | 0.82 | 256 |
| 345 | 1.48 | 0.70 | 0.80 | 210 |
| 375 | 1.41 | 0.72 | 0.79 | 132 |
| 405 | 1.29 | 0.75 | 0.78 | 87 |

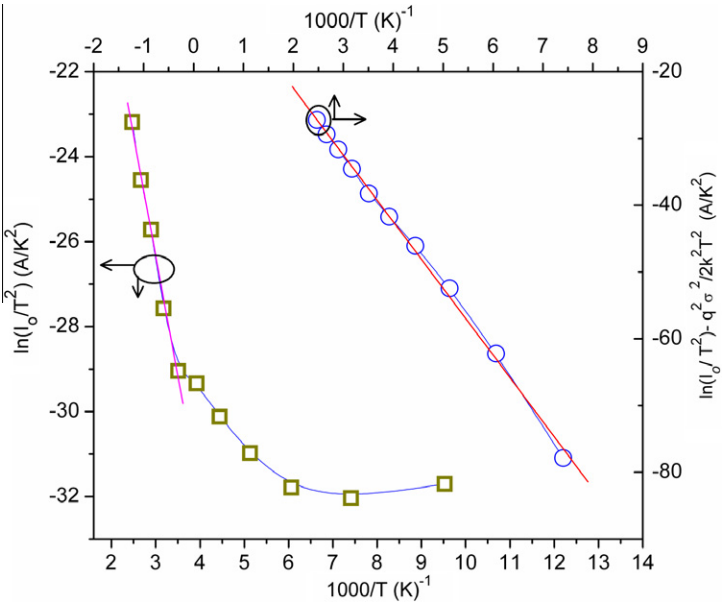


**Fig. 4.** Conventional Richardson plot of the $\ln(I_o/T^2)$ versus 1000/T (open squares) and modified Richardson $\ln(I_0/T^2)$-$(q^2\sigma_0^2/2k^2T^2)$ versus 1000/T plots for the Ru/Pd/n-GaN Schottky contact according to the Gaussian distribution of barrier heights. The open circles represent the plot calculated for $\sigma_0 = 0.111$ V. The straight line indicates the best fitting of the data in the temperature ranges 105–405 K.

neities [45]. The barrier inhomogeneities can arise from the different interface quality, which, in turn, depends on several factors such as the surface defects density, the surface treatment (cleaning, etching, etc.), the metal and the deposition process [45,46]. Schmitsdorf et al. [47] used Tung's theoretical approach and found a linear correlation between the experimental zero-bias barrier height $\Phi_{bo}$ and the ideality factor $n$. A plot of the experimental barrier height versus ideality factor is shown in Fig. 5. The straight line in Fig. 5, is the least squares fit to the experimental data. As can be seen from Fig. 5, there is a linear relationship between the experimental effective barrier heights and the ideality factors of the Ru/Pd/n-GaN Schottky contact that is explained by lateral inhomogeneities of the barrier heights in the Schottky diodes [47]. The extrapolation of the experimental barrier heights versus ideality factor plot to $n = 1$ has given a homogeneous BH of approximately 0.76 eV. This homogeneous barrier height value (0.76 eV) is in close agreement with 0.74 eV obtained by Siva Pratap Reddy et al. [20] on the Ni/Pd/n-GaN Schottky barrier diode.

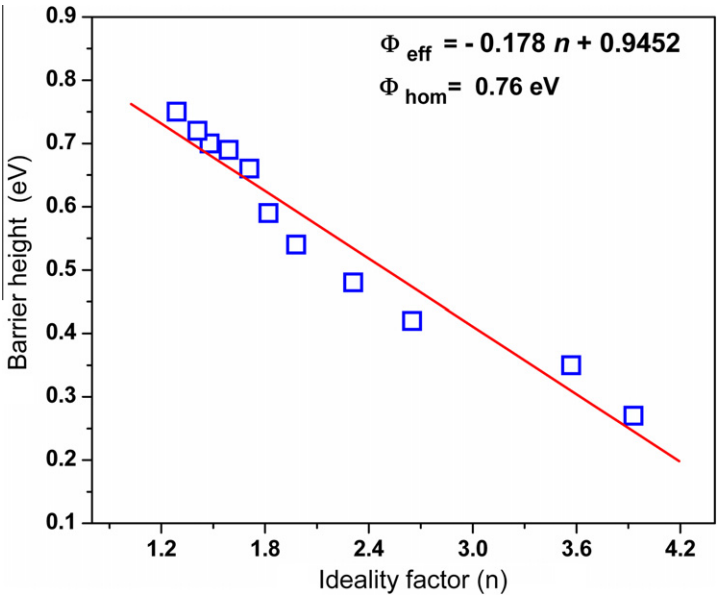


**Fig. 5.** Zero-bias apparent barrier height versus ideality factor of Ru/Pd/n-GaN Schottky diode at different temperatures.

In order to describe the abnormal behavior of the *I–V* characteristics (zero-bias barrier height, ideality factor and Richardson's constant), Song et al. [48] introduced an analytical potential fluctuation model based on spatially inhomogeneous barrier heights at the interface [48,49]. Let us assume that the distribution of the barrier heights is a Gaussian distribution of the barrier heights with a mean value $\bar{\Phi}_b$ and a standard deviation $\sigma_s$ in the form of [48,49]

$$P(\Phi_b) = \frac{1}{\sigma_s\sqrt{2\pi}} \exp\left(-\frac{(\Phi_b - \bar{\Phi}_b)^2}{2\sigma_s^2}\right) \tag{7}$$

The total current in a given forward bias $V$ is then given by

$$I(V) = \int_{-\infty}^{+\infty} I(\Phi_b, V) P(\Phi_b) d\Phi \tag{8}$$

Upon integration,

$$I(V) = A^* T^2 \exp\left[-\frac{q}{kT}\left(\bar{\Phi}_b - \frac{q\sigma_s^2}{2kT}\right)\right] \exp\left(\frac{qV}{n_{ap}kT}\right)\left[1 - \exp\left(\frac{-qV}{kT}\right)\right] \tag{9}$$

with

$$I_0 = AA^*T^2 \exp\left(\frac{-q\Phi_{ap}}{kT}\right) \tag{10}$$

where $\Phi_{ap}$ and $n_{ap}$ are the apparent barrier height and apparent ideality factor, respectively, and are given by

$$\Phi_{ap} = \bar{\Phi}_{b0}(T = 0) - \frac{q\sigma_0^2}{2kT} \tag{11}$$

$$\left(\frac{1}{n_{ap}} - 1\right) = \rho_2 - \frac{q\rho_3}{2kT} \tag{12}$$

It is assumed that the mean SBH $\bar{\Phi}_b$ and $\sigma_s$ are linearly bias dependent on Gaussian parameters such as $\bar{\Phi}_b = \bar{\Phi}_{bo} + \rho_2 V$ and standard deviation $\sigma_s^2 = \sigma_{so}^2 + \rho_3 V$,where $\rho_2$ and $\rho_3$ are voltage coefficients which may depend on temperature and they quantify the voltage deformation of the barrier height distribution. The temperature dependence of $\sigma_s$ is usually small and can be neglected [50].

Fitting of the experimental data into Eqs. (2), (10) and in Eq. (3) gives $\Phi_{ap}$ and $n_{ap}$ respectively, which should obey Eqs. (11) and (12). Thus, the plot of $\Phi_{ap}$ versus $1/2kT$ (Fig. 6) should be a straight line that gives $\bar{\Phi}_{bo}$ ($T = 0$) and $\sigma_o$ from the intercept and slope, respectively. The values of 0.89 eV and 111 mV for $\bar{\Phi}_{bo}$ ($T = 0$) and $\sigma_o$, respectively, are extracted from the least-square linear fitting of the data. Moreover, as can be seen in Fig. 2, the experimental results of $\Phi_{ap}$ fit very well with theoretical Eq. (11) with $\bar{\Phi}_{bo} = 0.89$ eV and $\sigma_o = 111$ mV. The solid line in Fig. 2 represents data estimated with these parameters using Eq. (11). When comparing $\bar{\Phi}_{bo}$ and $\sigma_o$ parameters, it is seen that the standard deviation is 12.4% of the mean barrier height. The standard deviation is a measure of the barrier homogeneity. There is no standard deviation for a homogeneous Schottky contact and hence the $\Phi_{ap}$ versus $1/2kT$ plot should be just a horizontal line. However, if inhomogeneities exist and are represented by a Gaussian distribution of barrier heights, the straight line tilts from the horizontal which corresponds to a negative slope and becomes progressively steeper with increasing $\sigma_o$ [17]. For our diodes, the obtained value of the standard deviation $\sigma_o$ is 111 mV which indicates the significant barrier inhomogeneity. This is responsible for the non-linearity of the $\Phi_{ap}$ versus $1/2kT$ plot. The lower value of $\sigma_o$ corresponds to a more homogeneous barrier height. It is seen that the value of $\sigma_o = 111$ mV is not small compared to the mean value of $\bar{\Phi}_{bo}$ ($T = 0$) = 0.89 eV, and it indicates greater inhomogeneities at the interface of our Ru/Pd/n-GaN device. As clearly stated in Refs. [48,49], barrier inhomogeneities can occur as a result of inhomogeneities in the composition of the interfacial oxide layer, non-uniformity of interfacial charges and interfacial oxide layer thickness. Therefore, low temperature $I$–$V$ characteristics are affected by this inhomogeneity and potential fluctuation. Particularly it is responsible for the curved behavior in the Richardson plot in Fig. 4 [48–50].

Fig. 6 shows the $(n^{-1}-1)$ versus $1/2kT$ plot. According to Eq. (12), this plot should be a straight line that gives the voltage coefficients $\rho_2$ and $\rho_3$ from the intercept and slope, respectively. The values of $\rho_2 = -0.132$ V and $\rho_3 = 0.012$ V are deduced from the experimental $(n^{-1}-1)$ versus $1/2kT$ plot. The linear behavior of the $(n^{-1}-1)$ versus $1/2kT$ plot confirms that the ideality factor does indeed denote the voltage deformation of the Gaussian distribution of the BH. Furthermore, the experimental results of

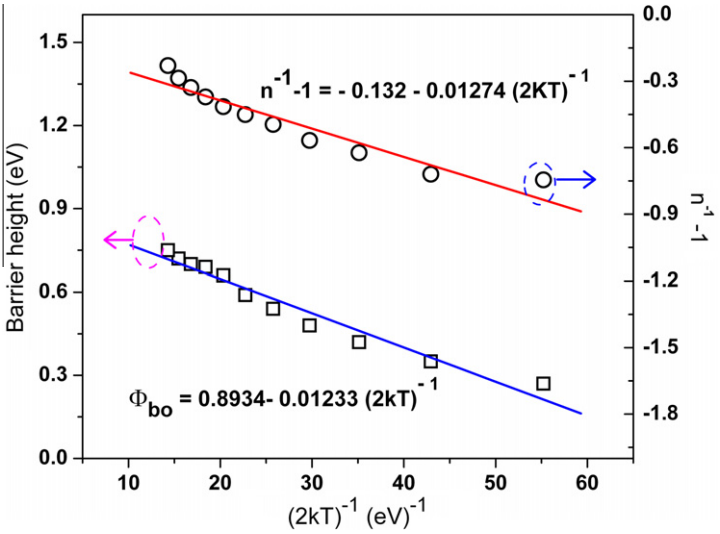


**Fig. 6.** Zero-bias apparent barrier height and ideality factor versus $1/2kT$ plots and their linear fits for the Ru/Pd/n-GaN Schottky barrier diode according to Gaussian distribution of the barrier heights.

$n_{ap}$ fit very well with Eq. (12) with $\rho_2 = -0.132$ V and $\rho_3 = 0.012$ V. The continuous solid line in Fig. 2 represents data estimated with these parameters using Eq. (12).

The conventional Richardson plot (open squares in Fig. 4) based on the thermionic emission current mechanism has showed nonlinearity at low temperatures. By considering Eqs. (2) and (11), an expression for the modified Richardson plot according to the Gaussian distribution of the barrier heights can be written as

$$\ln\left(\frac{I_0}{T^2}\right) - \left(\frac{q^2\sigma_0^2}{2k^2T^2}\right) = \ln(AA^*) - \frac{q\bar{\Phi}_{b0}}{kT} \tag{13}$$

Using the experimental $I_o$ data, the modified $\ln(I_0/T^2) - (q^2\sigma_0^2/2k^2T^2)$ versus 1000/T plot can be obtained according to Eq. (13). This plot should give a straight line with slope directly yielding the mean barrier $\bar{\Phi}_{bo}$ and the intercept ($\ln AA^*$) at the ordinate determining $A^*$ for a given diode area A. The $\ln(I_0/T^2)$-$(q^2\sigma_0^2/2k^2T^2)$ values are calculated using the value of $\sigma_o$ obtained from the $\Phi_{ap}$ versus 1/2 kT plot (Fig. 6). Thus, the open circles in Fig. 4 have given the modified $\ln(I_0/T^2)$-$(q^2\sigma_0^2/2k^2T^2)$ versus 1000/T plot for the value of $\sigma_o$ = 111 mV. As can be seen from Fig. 4, the modified Richardson plot has a quite good linearity over the whole temperature range corresponding to single activation energy around $\bar{\Phi}_{bo}$. The best linear fitting to these modified experimental data is depicted by the solid line in Fig. 4 which represents the true activation energy plots in the temperature range of 105–405 K. A zero-bias mean BH $\bar{\Phi}_{bo}$ of 0.87 eV has been obtained from this plot. This value is in close agreement with the value of 0.89 eV obtained from the $\Phi_{ap}$ versus 1/2 kT plot (Fig. 6). The intercept at the ordinate of the modified $\ln(I_0/T^2)$-$(q^2\sigma_0^2/2k^2T^2)$ versus 1000/T plot gives the Richardson constant $A^*$ as 21.25 $Acm^{-2}K^{-2}$ without using the temperature coefficient of the BHs. The obtained Richardson constant value is in close agreement with the theoretical value of 26.4 $Acm^{-2}\,K^{-2}$ for n-GaN.

### 3.2. Temperature-dependent capacitance–voltage (C–V) characteristics

The experimental reverse-bias $C^{-2}$–V characteristics of the Ru/Pd/n-GaN SBD in the temperature range of 105–405 K in steps of 30 K are shown in Fig. 7. *C–V* measurements are performed at a frequency of 1 MHz. In Schottky diodes, the depletion layer capacitance can be expressed as [27]

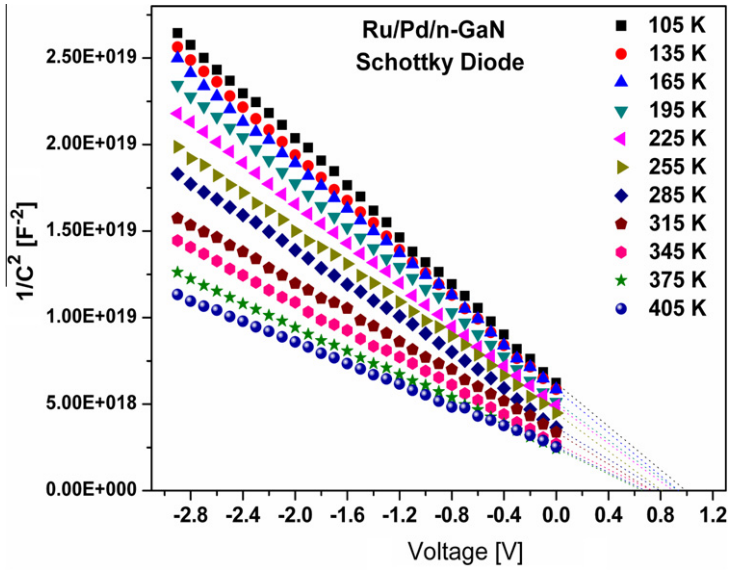


**Fig. 7.** The reverse bias $C^{-2}$–V characteristics of the Ru/Pd/n-GaN Schottky barrier diode at various temperatures.

$$\frac{1}{C^2} = \left[\frac{2(V_{bi} + V - kT/q)}{qN_d\varepsilon_s A^2}\right] \tag{14}$$

where $A$ is the Schottky contact area, $V_{bi}$ is the diffusion potential, $V$ is the reverse bias voltage and $N_d$ is the carrier concentration obtained from the slope of the reverse bias $C^{-2}$–V plot. From Eq. (14), the slope of the reverse-bias $C^{-2}$–V curves is given by

$$\frac{d(C^{-2})}{dV} = \frac{2}{qN_d\varepsilon_s A^2} \tag{15}$$

The diffusion potential $V_{bi}$ is determined from the extrapolation of the linear $C^{-2}$–V plot to the $v$-axis, and is given by the Eq. $V_{bi} = V_o + kT/q$, where $V_o$ is the x-intercept and $T$ is the absolute temperature. The barrier height deduced from the $C^{-2}$–V curves is then obtained from

$$\Phi_{C-V} = V_{bi} + V_n \tag{16}$$

where $V_n$ is the potential difference between the Fermi level and minimum of the conduction band for n-GaN in the neutral region, and it can be calculated from the following Eq.

$$V_n = \frac{kT}{q}\ln\left[\frac{N_c}{N_d}\right] \tag{17}$$

where $N_c$ is the state density in the conduction band for n-GaN, $N_c = 2.53 \times 10^{18}$ cm$^{-3}$ at room temperature and has a temperature dependence of $N_{c\alpha}T^{3/2}$.

The temperature dependence of the experimental carrier concentration ($N_d$) is calculated from the reverse-bias $C^{-2}$–V characteristics. A plot between $N_d$ and 1000/T is shown in Fig. 8. The estimated values of $N_d$ are $2.21 \times 10^{17}$ and $4.13 \times 10^{17}$ cm$^{-3}$ for the n-GaN wafer at 105 and 405 K. As can be seen from Fig. 8, the carrier concentration of the n-GaN slightly decreases with a decrease in temperature. At very low temperatures, most impurities are frozen out. It is also noted form Fig. 8 the carrier concentration increases with temperature and that it becomes very sensitive to temperatures at temperatures about 255 K. This is due to the fact that almost all the donors are ionized and the deep level traps emit more electrons with an increase in temperature, and thus the carrier concentration increases [45].

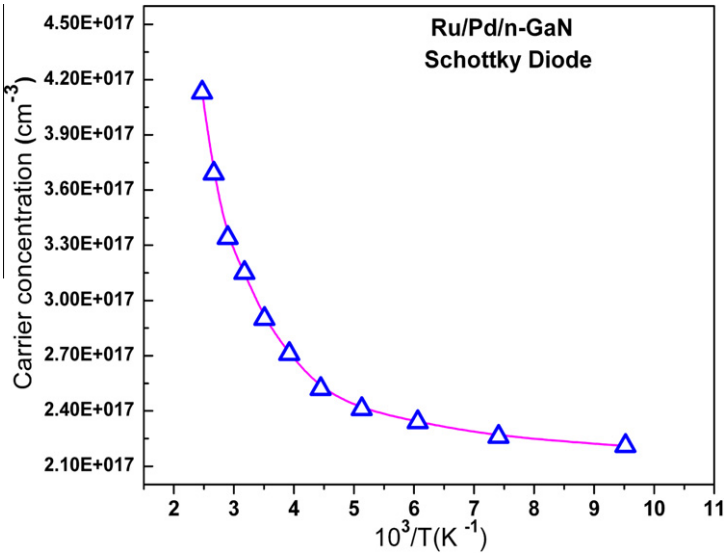


**Fig. 8.** Temperature dependence of the carrier concentration obtained from the experimental reverse bias $C^{-2}$–V characteristics (Fig. 7) for typical Ru/Pd/n-GaN Schottky diode.

As can be seen from the Table 1, the barrier heights obtained from *C–V* measurements are higher than those obtained from *I–V* measurements. The difference in barrier heights obtained from *I–V* and *C–V* measurements is attributed to the interface states due to the intervening insulating layer, contaminations in the interfaces, fixed surface polarization charges, deep impurity levels, edge leakage current and nitride-related other defects [51]. According to Tung [34,36], the discrepancy between barrier heights measured by different techniques might be associated with the instrumentation problems, that is, the way to determine true space charge capacitance from *C–V* data or a large series resistance, which could affect the value determined from *I–V* data.

The temperature dependent experimental values of $N_d$ and $N_c$ are used in calculating the values of $\Phi_{C-V}$ using Eq. (16). The barrier height ($\Phi_{C-V}$) versus temperature ($T$) plot is drawn (Fig. 2) from the $C^{-2}$–V characteristics for Ru/Pd/n-GaN Schottky diode in the temperature range 105–405 K. The values of $\Phi_{C-V}$ are ranges from 1.02 eV at 105 K to 0.78 eV at 405 K. The temperature dependence of the $\Phi_{C-V}$ can be fitted with $\Phi_{C-V} = \Phi_{C-V}(T = 0)+\alpha T$ [50], where $\Phi_{C-V}(T = 0\ \mathrm{K})$ and $\alpha$ represents the barrier height extrapolated to the absolute zero and the temperature coefficient of the $\Phi_{C-V}$, respectively. The fit of the $\Phi_{C-V}$ data with this expression gives $\alpha = -0.942$ meV/K and $\Phi_{C-V}(T = 0)$=1.09 eV. The BH $\Phi_{C-V}$ from the $C^{-2}$–V decreases as the temperature increases. Generally, the variation of the barrier height due to the temperature should follow almost the variation of the semiconductor band gap as the temperature coefficient of the $\Phi_{C-V}$ nearly equals to that of the band gap of GaN [45,52]. The BH temperature coefficient of $\alpha = -0.942$ meV/K is in close agreement with temperature coefficient $-1.08$ meV/K of the band gap [52]. That is, such a temperature dependence implies the Fermi level is pinned to the bottom of the valence band at the MS interface due to defects [45,52].

### 3.3. Determination of interface states density

Usually a thin insulating interfacial layer is always present between semiconductor crystal and metal [53,54] due to incomplete covalent bonds, chemical reaction and sharp discontinuity, which results in a new dielectric phase. The mere existence of an electric charge in the thin interfacial layer, which is neither semiconductor nor metal, introduces a high density of interface states [53,55]. Therefore, the expression for the density of interface states as deduced by Card and Rhoderick [56] is reduced to

$$N_{ss}(V) = \frac{1}{q}\left[\frac{\varepsilon_i}{\delta}(n(V) - 1) - \frac{\varepsilon_s}{W_D}\right] \tag{18}$$

here $\varepsilon_i$ is the permittivity of the interfacial layer, $W_D$ is the width of the space charge region extracted from the experimental *C–V* data using Eq. (19) and $\delta$ is the thickness of the interfacial layer extracted from Eq. (20). The voltage-dependent ideality factor $n(V)$ has been extracted from Eq. (21)

$$W_D = \sqrt{\frac{2\varepsilon_S V_{bi}}{qN_d}} \tag{19}$$

$$\frac{\varepsilon_i}{A} = \frac{\varepsilon_i \varepsilon_o}{\delta} \tag{20}$$

$$n(V) = \frac{qV}{kT\ln(I/I_O)} \tag{21}$$

Furthermore, taking into account the bias dependent effective barrier height and the energy of the interface states with respect to the conduction band edge ($E_C$–$E_{SS}$) are obtained by Eqs. (22) and (23) as follows [57]

$$\Phi_e = \Phi_{bo} + \left(1 - \frac{1}{n(V)}\right)V \tag{22}$$

$$E_C - E_{SS} = q(\Phi_e - V) \tag{23}$$

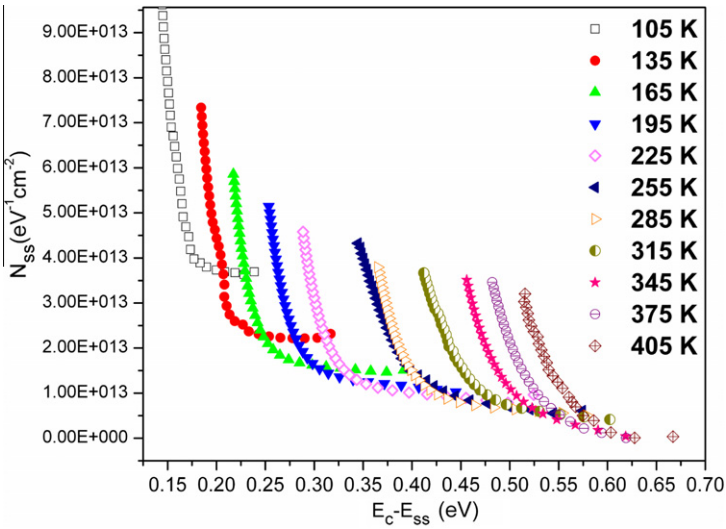


**Fig. 9.** Density of interface states $N_{SS}$ as a function of $E_C$–$E_{SS}$ for the Ru/Pd/n-GaN Schottky diode at various temperatures.

The energy density distribution profiles of the interface states ($N_{SS}$) for Ru/Pd/n-GaN Schottky barrier diodes are extracted from the experimental forward-bias *I–V* characteristics (Fig. 1). A plot between $N_{SS}$ and $E_C$–$E_{SS}$ is shown in Fig. 9. It is clearly seen from Fig. 9 that $N_{SS}$ has an exponential growth from midgap of GaN towards to bottom of conduction band and increase with decreasing temperature. Such behavior of $N_{SS}$ has been explained with variation of the ideality factor as a function of temperature due to lateral inhomogeneities of the barrier height at the metal–semiconductor interface [58]. Moreover, as seen in Fig. 9, the energy values of the density distribution of $N_{SS}$ are in the range $E_C$-0.14 eV to $E_C$-0.23 eV at 105 K and $E_C$-0.51 eV to $E_C$-0.66 eV at 405 K. At 105 K, the magnitude of the interface state density ($N_{SS}$) is varied from $3.58 \times 10^{13}$ $eV^{-1}cm^{-2}$ ($E_C$-0.23 eV) to $9.38 \times 10^{13}$ $eV^{-1}cm^{-2}$ ($E_C$-0.14 eV). Also, at 405 K, the magnitude of the interface state density ($N_{SS}$) is varied from $1.06 \times 10^{12}eV^{-1}cm^{-2}$ ($E_C$-0.66 eV) to $3.20 \times 10^{13}$ $eV^{-1}cm^{-2}$ ($E_C$-0.51 eV). The interface state density values calculated for the Ru/Pd/n-GaN are in well agreement with those reported in the literature [12,57]. The non-uniform distribution of $N_{SS}$ ($E$) is supposed to be due to the presence of discrete deep levels which are associated to the residual defects in the as-grown GaN films which are usually believed to be positioned away from the metal–semiconductor interface. In such case, the interfacial layer separating the metal from the defects is the semiconductor itself. Thus, the density of deep levels associated to native defects is supposed to peak at the energetic positions of the defect with respect to the band edge of the GaN film. This in turn indicates that the non-uniform distribution of the density of deep defects introduces a non-uniform lateral distribution of gap states at the metal/GaN interface. Accordingly, the density of surface states associated to defects will peak at the energy positions of these defects [12].

### *3.4. Deep level transient spectroscopy of Ru/Pd/n-GaN Schottky diode*

Deep level transient spectroscopy (DLTS) is one of the most sensitive tools for detection and characterization of electrically active defects in a semiconductor thin film Schottky junction device structure [21]. DLTS measurements are performed over the temperature range 105–405 K using automated DLTS system. Typically, a quiescent reverse bias of $V_r = -1$ V was employed with filling-pulse voltage $V_p = +0.5$ V and filling pulse width $t_p = 100$ μs. Any deep level can be experienced as either capture or emission of carrier, with transition probabilities per unit time depending on the free carrier concentrations, capture cross-section of the trap, ionization energy and temperature. According to the value

of applied voltage for the electron trap studied here in the space charge zone of Schottky diode on n-type GaN in the dark, either emission or capture of electrons toward or from the bottom $E_C$ of the conduction band is relevant. When the Fermi level just coincides with the trap level $E_T$, the capture coefficient equals the emission rate $e_n$ resulting at equilibrium which is given by [59]

$$e_n = \sigma_n V_{th} N_C \exp\left(\frac{E_T - E_C}{kT}\right) = \frac{1}{\tau_e} \tag{24}$$

here $\sigma_n$ is the capture cross-section, $V_{th}$ is the thermal velocity of an electron defined as $v_{th} = (3kT/m_{eff})^{1/2}$, $N_C$ is the effective density of states at the bottom of the conduction band, $k$ is the Boltzmann's constant, $T$ is the absolute temperature and $\tau_e$ is the emission time constant, which is the reciprocal of the emission rate $e_n$. The DLTS spectrum of as-deposited Ru/Pd Schottky diode which is measured with lock-in frequency of 42 Hz is shown in Fig. 10. The DLTS spectrum reveals two deep level defects in the as-grown GaN layer and are labeled as '$E_1$' and '$E_2$'. It is obvious that the peak $E_1$ seems to be too broad. The broad feature of the peak $E_1$ might be the result of the superposition of DLTS signals of several different trap levels [60] or consist of multiple levels [61].

The thermal activation energy for electron emission from each deep level is determined from an Arrhenius analysis of the emission time constant. From several such spectra, the product $e_n^{-1} v_{th} N_C$ can be calculated and plotted as function of 1000/T, leading usually to the straight line in an Arrhenius plot. Fig. 11 shows Arrhenius plot for the two deep levels $E_1$ and $E_2$. The estimated activation energies for trap $E_1$ = 0.54 eV at 328 K and trap $E_2$ = 0.68 eV at 374 K. The observed deep level $E_1$ in our sample with an activation energy of 0.54 eV which is similar to that reported by Hacke et al. [25] and Tokuda et al. [26] observed in Si-doped GaN grown by MOCVD. It is suggested that trap $E_1$ might be associated with $N_{Ga}$-related defect [26]. Finally is our deep level $E_2$ as corresponding to the 0.68 eV level is fairly similar to those observed by Wang et al. [23], showing a defect level at 0.65 eV in n-GaN grown by reactive MBE and by Hacke et al. [25], showing a defect at 0.66 eV in HVPE grown GaN. These defects ($E_1$ and $E_2$) have been correlated with as-grown defects reported by Hacke et al. in n-GaN grown by HVPE [25] and by Gotz et al. in MOCVD-grown GaN [24].

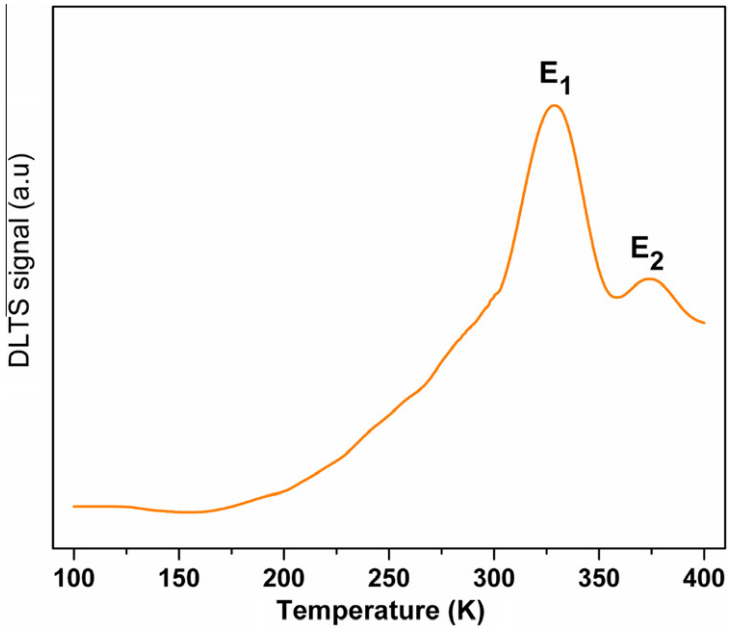


**Fig. 10.** The DLTS spectrum of Pd/Ru Schottky contact on as-grown n-type GaN ($Vr$ = −1 V, $Vp$ = +0.5 V, $t_p$ = 100 μs, $f$ = 42 Hz).

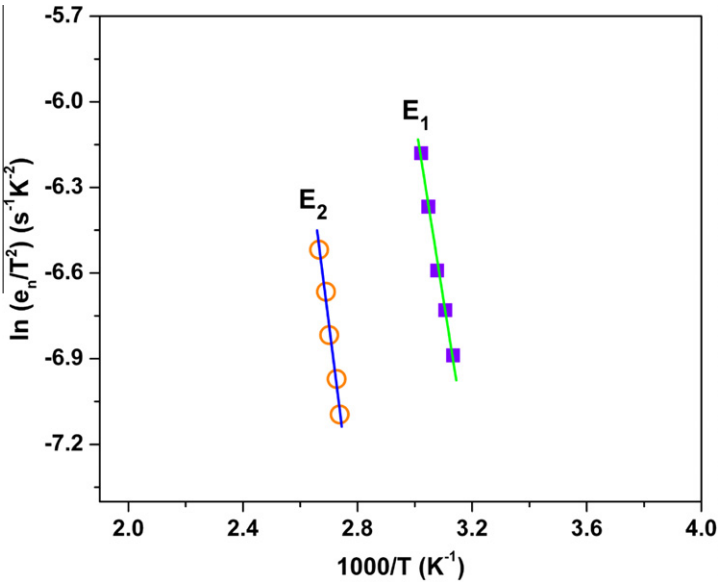


**Fig. 11.** Arrhenius plot of emission rate and temperature for the two deep level defects in Ru/Pd/n-GaN Schottky diode.

## 4. Conclusion

In conclusion, we have discussed current transport mechanisms in Ru/Pd/n-GaN Schottky barrier diodes in the temperature range from 105 K to 405 K. Using thermionic emission theory, the calculated *I–V* barrier heights and ideality factors are range from 0.27 eV and 3.93 at 105 K to 0.75 eV and 1.29 at 405 K, respectively. It is observed that the ideality factor increases and barrier height decreases with decrease in temperature. This can be explained on the basis of thermionic emission with Gaussian distribution of the barrier heights. The estimated values of series resistance ($R_s$) from Cheung's method are in the range of 1027 Ω at 105 K to 87 Ω at 405 K. A modified $\ln(I_0/T^2)$-$(q^2\sigma_0^2/2k^2T^2)$ versus 1000/T plot gives mean barrier height $\bar{\Phi}_{bo}$ and Richardson constant A* as 0.87 eV and 21.25 A/cm$^2$ K$^2$. The estimated Richardson constant value is in close agreement with the known value of 26.4 A/cm$^2$ K$^2$ for n-type GaN. The discrepancy between Schottky barrier height estimated from *I–V* and *C–V* measurements is also discussed. The homogeneous Schottky barrier height value is approximately 0.76 eV for the Ru/Pd/n-GaN Schottky barrier diodes which is deduced from the linear relationship between the experimental barrier heights and ideality factor. The energy distribution profile of $N_{SS}$ is obtained from the forward bias *I–V* characteristics by taking into account the bias dependence of the effective barrier height ($\Phi_e$) and ideality factor ($n(V)$). It is found that the $N_{SS}$ values decrease with an increase in temperature (from $9.38 \times 10^{13}$ eV$^{-1}$ cm$^{-2}$ at 105 K to $1.06 \times 10^{12}$ eV$^{-1}$ cm$^{-2}$ at 405 K). DLTS measurements revealed the presence of two deep level defects with activation energies $E_1$ = 0.54 eV and $E_2$ = 0.68 eV, suggest that the deep level $E_2$ most probably associated with $N_{Ga}$-related defect.

## References

[1] S.J. Pearton, C.R. Abernathy, F. Ren, Gallium Nitride Processing for Electronics, Sensors and Spintronics, Springer-Verlag, London, 2006.
[2] M.A. Khan, J.N. Kuznia, D.T. Olson, M. Blasingame, A.R. Bhattarai, Appl. Phys. Lett. 63 (1993) 2455.
[3] J. Pankove, S.S. Chang, H.C. Lee, R.J. Molnar, T.D. Moustakas, B. Van Zeghbroeck, Tech. Dig., Int. Electron Devices Meet. 94 (1994) 389.
[4] S. Nakamura, T. Mukai, M. Senoh, Appl. Phys. Lett. 64 (1994) 28.
[5] M.A. Khan, J.N. Kuznia, A.R. Bhattarai, D.T. Olson, Appl. Phys. Lett. 62 (1993) 1786.

[6] M.A. Khan, A.R. Bhattarai, J.N. Kuznia, D.T. Olson, Appl. Phys. Lett. 63 (1993) 1214.
[7] F. Iucolano, F. Roccaforte, F. Giannazzo, V. Raineri, Appl. Phys. Lett. 98 (2007) 092119.
[8] S. Huang, B. Shen, M.J. Wang, F.J. Xu, Y. Wang, H.Y. Yang, F. Lin, L. Lu, Z.P. Chen, Z.X. Qin, Z.J. Yang, G.Y. Zhang, Appl. Phys. Lett. 91 (2007) 072109.
[9] A.T. Ping, A.C. Schmitz, M. Asif Khan, I. Adesida, Electron. Lett. 32 (1996) 68.
[10] V. Rajagopal Reddy, M. Ravinandan, P. Koteswara Rao, C.-J. Choi, J. Mater. Sci: Mater. Electron. 20 (2009) 1018.
[11] M. Diale, F.D. Auret, Physica B 404 (2009) 4415.
[12] M. Mamor, J. Phys:Condens. Matter. 21 (2009) 335802.
[13] F.E. Cimilli, M. Saglam, H. Efeoglu, A. Turut, Physica B 404 (2009) 1558.
[14] M.E. Aydin, T. Kilicoglu, K. Akkilic, H. Hasgoren, Physica B 381 (2006) 113.
[15] M.E. Aydin, K. Akkilic, T. Kilicoglu, Appl. Surf. Sci. 253 (2006) 1304.
[16] Z. Benamara, B. Akkal, A. Talbi, B. Gruzza, Mater. Sci. Eng. C 26 (2006) 519.
[17] S. Dogan, S. Duman, B. Gurbulak, S. Tuzemen, H. Morkoc, Physica E 41 (2009) 646.
[18] S. Suresh, M. Balaji, V. Ganesh, K. Baskar, J. Alloys Compd. 506 (2010) 615.
[19] W. Mtangi, P.J.J.V. Rensburg, M. Diale, F.D. Auret, C. Nyamhere, J.M. Nel, A. Chawanda, Mater. Sci. Eng. B 171 (2010) 1.
[20] M. Siva Pratap Reddy, A. Ashok Kumar, V. Rajagopal Reddy, Thin Solid Films 519 (2011) 3844.
[21] P.K. Rao, B. Park, S.-T. Lee, Y.-K. Noh, M.-D. Kim, J.-E. Oh, J. Appl. Phys. 110 (2011) 013716.
[22] A. Hierro, D. Kwon, S.A. Ringel, M. Hansen, J.S. Speck, U.K. Mishra, S.P. DenBaars, Appl. Phys. Lett. 76 (2000) 3064.
[23] C.D. Wang, L.S. Yu, S.S. Lau, E.T. Yu, W. Kim, A.E. Botchkarev, H. Morkoc, Appl. Phys. Lett. 72 (1998) 1211.
[24] W. Gotz, N.M. Johnson, H. Amano, I. Akasaki, Appl. Phys. Lett. 65 (1994) 463.
[25] P. Hacke, T. Detchprohm, K. Hiramatsu, N. Sawaki, K. Tadatomo, K. Miyake, J. Appl. Phys. 76 (1994) 304.
[26] Y. Tokuda, Y. Matsuoka, H. Ueda, O. Ishiguro, N. Soejima, T. Kachi, Superlattices Microstruct. 40 (2006) 268.
[27] E.H. Rhoderick, R.H. Williams, Metal-Semiconductor contacts, Clarendon, Oxford, 1988.
[28] Li. Fei, Z.X. -Ling, D. Yi, X.X. -Song, L.C. -Zhi, Chin. Phys. B 18 (2009) 5029.
[29] T. Hashizume, T. Kotani, H. Hasegawa, Appl. Phys. Lett. 84 (2004) 4884.
[30] E.J. Miller, E.T. Yu, P. Waltereit, J.S. Speck, Appl. Phys. Lett. 84 (2004) 535.
[31] B. Akkal, Z. Benamara, H. Abid, A. Talbi, B. Gruzza, Mater. Chem. Phys. 85 (2004) 27.
[32] R. Singh, S.K. Arora, R. Tyagi, S.K. Agarwal, D. Kanjilal, Bull. Mater. Sci. 23 (2000) 471.
[33] R.T. Tung, Appl. Phys. Lett. 58 (1991) 2821.
[34] R.T. Tung, Mater. Sci. Eng. R 35 (2001) 1.
[35] F.A. Padovani, G. Summer, Appl. Phys. A 36 (1965) 3744.
[36] R.T. Tung, Phys. Rev. B 45 (1992) 13509.
[37] S. Karatas, S. Altindal, Mater. Sci. Eng. B 122 (2005) 133.
[38] A. Turut, M. Saglam, H. Efeoglu, N. Yalcin, M. Yildirim, B. Abay, Physica B 205 (1995) 41.
[39] S.K. Cheung, N.W. Cheung, Appl. Phys. Lett. 49 (1986) 85.
[40] S. Chand, J. Kumar, Appl. Phys. A 63 (1996) 171.
[41] P. Hacke, T. Detchprohm, K. Hiramatsu, N. Sawaki, Appl. Phys. Lett. 63 (1993) 2676.
[42] J.D. Guo, M.S. Feng, R.J. Guo, F.M. Pan, C.Y. Chang, Appl. Phys. Lett. 67 (1995) 2657.
[43] M.C. Lonergan, F.E. Jones, J. Chem. Phys. 115 (2001) 433.
[44] S. Zhu, R.L. Van Meirhaeghe, S. Forment, G.P. Ru, X.P. Qu, B.Z. Li, Solid-State Electron. 48 (2004) 1205.
[45] N. Yildirim, K. Ejderha, A. Turut, J. Appl. Phys. 108 (2010) 114506.
[46] J.P. Sullivan, R.T. Tung, M.R. Pinto, W.R. Graham, J. Appl. Phys. 70 (1991) 7403.
[47] R.F. Schmitsdorf, T.U. Kampen, W. Monch, Surf. Sci. 324 (1995) 249.
[48] Y.P. Song, R.L. Van Meirhaeghe, W.H. Laflere, F. Cardon, Solid-State Electron. 29 (1986) 633.
[49] C.A. Dimitriadis, S. Logothetidis, I. Alexandrou, Appl. Phys. Lett. 66 (1995) 502.
[50] S. Zhu, R.L. Van Meirhaeghe, C. Detavernier, F. Cardon, G.P. Ru, X.P. Qu, B.Z. Li, Solid-State Electron. 44 (2000) 663.
[51] J. Pedros, R. Cuerdo, R. Lossy, N. Chaturvedi, J. Wurfl, F. Calle, Phys. Status Solidi C 3 (2006) 1709.
[52] C. Lu, S.N. Mohammad, Appl. Phys. Lett. 89 (2006) 162111.
[53] B.G. Streetman, S.K. Banerjee, Solid state Electronic Devices, 6th ed., Englewood Cliffs, NJ: Prentice –Hall, 2006.
[54] L.J. Brillson, Mater. Sci. Eng. 75 (2000) 218.
[55] A. Geotzberger, V. Heine, E.H. Nicollian, Appl. Phys. Lett. 12 (1968) 95.
[56] H.C. Card, E.H. Rhoderick, J. Phys. D: Appl. Phys. 4 (1971) 1589.
[57] S.M. Faraz, H. Ashraf, M.I. Arshad, P.R. Hageman, M. Asghar, Q. Wahab, Semicond. Sci. Technol. 25 (2010) 095008.
[58] N. Ucar, A.F. Ozdemir, D.A. Aldemir, S. Cakmak, A. Calik, H. Yildiz, F. Cimilli, Superlattices Microstruct. 47 (2010) 586.
[59] P. Muret, Ch. Ulzhofer, J. Pernot, Y. Cordier, F. Semond, Ch. Gacquiere, D. Theron, Superlattices Microstruct. 36 (2004) 435.
[60] C.B. Soh, D.Z. Chi, A. Ramam, H.F. Lim, S.J. Chua, Mater. Sci. Semicond. Process. 4 (2001) 595.
[61] Z.-Q. Fang, J.W. Hemsky, D.C. Look, M.P. Mack, Appl. Phys. Lett. 72 (1998) 448.